Plutonium Oxidation and Subsequent Reduction by Mn(IV) Minerals in Yucca Mountain Tuff

ARTICLE *in* ENVIRONMENTAL SCIENCE AND TECHNOLOGY · JULY 2006

Impact Factor: 5.33 · DOI: 10.1021/es052353+ · Source: PubMed

Environ. Sci. Technol. **2006**, *40,* 3508−3514

Plutonium Oxidation and Subsequent Reduction by Mn(IV) Minerals in Yucca Mountain Tuff

BRIAN A. POWELL,*,† MARTINE C. DUFF,‡ DANIEL I. KAPLAN,‡ ROBERT A. FJELD,† MATTHEW NEWVILLE,§ DOUGLAS B. HUNTER,‡ PAUL M. BERTSCH,⊥ JOHN T. COATES,† PETER ENG,§ MARK L. RIVERS,§ STEVEN M. SERKIZ,‡ STEPHEN R. SUTTON,§ INES R. TRIAY,|| AND DAVID T. VANIMAN#

Department of Environmental Engineering and Science, Clemson University, Anderson, South Carolina 29630, Savannah River National Laboratory, Aiken, South Carolina 29808, Department of Geophysical Sciences and Center for Advanced Radiation Sources, The University of Chicago, Chicago, Illinois 60637, Savannah River Ecology Laboratory, The University of Georgia, Aiken, South Carolina 29808, Waste Isolation Pilot Plant, Carlsbad, New Mexico 88221, Los Alamos National Laboratory, Los Alamos, New Mexico 87545

Plutonium oxidation state distribution on Yucca Mountain tuff and synthetic pyrolusite (β-MnO_2) suspensions was measured using synchrotron X-ray micro-spectroscopy and microimaging techniques as well as ultrafiltration/solvent-extraction techniques. Plutonium sorbed to the tuff was preferentially associated with manganese oxides. For both Yucca Mountain tuff and synthetic pyrolusite, Pu(IV) or Pu-(V) was initially oxidized to more mobile Pu(V/VI), but over time, the less mobile Pu(IV) became the predominant oxidation state of the sorbed Pu. The observed stability of Pu-(IV) on oxidizing surfaces (e.g., pyrolusite), is proposed to be due to the formation of a stable hydrolyzed Pu(IV) surface species. These findings have important implications in estimating the risk associated with the geological burial of radiological waste in areas containing Mn-bearing minerals, such as at the Yucca Mountain or the Hanford Sites, because plutonium will be predominantly in a much less mobile oxidation state (i.e., Pu(IV)) than previously suggested (i.e., Pu(V/VI).

Introduction

The safe design of a radioactive waste or spent nuclear fuel repository requires an assessment of risks associated with the potential release of radionuclides into the surrounding environment. Knowledge of radionuclide geochemistry and the surrounding environment is required for predicting subsurface fate and transport. This task grows increasingly complicated for constituents such as Pu, which exhibit complex environmental chemistries. The environmental behavior of Pu can be influenced by complexation, precipitation, adsorption, colloid formation, microbial activity (e.g., direct interaction of biofilms or complexation with exerdates, such as siderophores), and oxidation/reduction (redox) reactions (*1*−*5*). The most important of these factors controlling Pu mobility is redox, more specifically, the oxidation state of Pu. This is because Pu(IV) is generally 2−3 orders of magnitude less mobile than Pu(V/VI) in most environments (*6*). Kaplan et al. (*7*) showed that Pu(IV) moved 10 cm through a vadose zone sediment, with >95% of the Pu remaining within 1.25 cm of the source, after 11 years of exposure to natural rainfall conditions at the Department of Energy (DOE) Savannah River Site (SRS). Pu oxidation and reduction reactions over the 11 year period were found to play an important role in Pu transport through the pH 6.1 system dominated with kaolinite, goethite, and hematite in the clay fraction. Oxidation was attributed to wet-dry cycling and its effects on Fe- and Mn-oxides and bacteria (*8*).

Pu commonly exists simultaneously in several oxidation states (*9*−*10*). Choppin (*11*) reported Pu may exist as Pu(IV), Pu(V), and/or Pu(VI) in oxic natural groundwaters. The pentavalent and hexavalent oxidation states of Pu are typically stabilized in aerated solutions (high E_H) and high pH (*12*). The most common assumed form of precipitated Pu in the environment is PuO_2(s) (*11*). The low solubility of PuO_2(s) generally limits subsurface mobility (although, enhanced transport of colloidal PuO_2 has been previously observed (*11, 13*−*14*)). Several researchers have observed that Pu adsorbed to solid surfaces is primarily Pu(IV) (*15*−*17*). Studies of Pu speciation in natural waters indicated that Pu associated with suspended particulate matter was Pu(IV), and aqueous phase Pu was predominantly Pu(V) (*12, 17*−*20*). Pu(IV) added to NaCl solutions, Gulf Stream water, or synthetic brines equilibrated as either Pu(V) or Pu(VI) within a few days (*1, 16, 21*). Based upon the observations described above, it has been generally accepted that, in natural systems, Pu associated with suspended particulate matter is predominantly Pu(IV), whereas Pu in the aqueous phase is predominantly Pu(V).

There are several mechanisms by which Pu may undergo an oxidation state transformation. Dissolved Pu may be oxidized by dissolved oxidants ($Cr_2O_7^{-2}$, MnO_4^-) or reduced by dissolved reductants (Fe^{2+}, natural organic matter). Plutonium oxidation state transformations may also be mediated by a solid phase. In these cases, a reduced species at the mineral surfaces may provide a direct electron source or the mineral phase may be a semiconductor, capable of providing a pathway for electron mobility.

The influence of the character of Mn-containing minerals expected to be found in subsurface repository environments on Pu oxidation state distributions has been the subject of much recent research. Kenney-Kennicutt and Morse (*15*), Duff et al. (*22*), and Morgenstern and Choppin (*23*) observed oxidation of Pu facilitated by Mn(IV)-bearing minerals. Conversely, Shaughnessy et al. (*24*) used X-ray absorption near-edge Structure (XANES) spectroscopy to show reduction of Pu(VI) by hausmannite ($Mn^{II}Mn^{III}_2O_4$) and manganite (γ-$Mn^{III}OOH$), and Kersting et al. (*13*) observed reduction of Pu(VI) by pyrolusite ($Mn^{IV}O_2$). In this paper, we attempt to reconcile the apparently conflicting datasets by showing that Mn-bearing minerals can indeed oxidize Pu; however, if the

* Corresponding author phone: (925) 422-0280 e-mail: powell37@llnl.gov. Current Address: Lawrence Livermore National Laboratory, Livermore, CA 94551.

† Department of Environmental Engineering and Science, Clemson University.

‡ Savannah River National Laboratory.

§ Department of Geophysical Sciences and Center for Advanced Radiation Sources, The University of Chicago.

⊥ Savannah River Ecology Laboratory, The University of Georgia.

|| Waste Isolation Pilot Plant, Carlsbad, NM.

Los Alamos National Laboratory.

10.1021/es052353+ CCC: $33.50
Published on Web 05/05/2006

oxidized species remains associated with the solid phase, the initial oxidation step is followed by reduction to Pu(IV), which over time becomes the predominant solid-phase Pu species. In this study, Pu sorbed to Yucca Mt. tuff (initial XANES and elemental mapping results were reported by Duff et al. (*22*)) were re-examined 2 years later. Additionally, time-dependent changes in the oxidation state distribution of Pu in synthetic pyrolusite suspensions were examined.

Materials and Methods

X-ray Absorption Spectroscopy. In a previous study, Duff et al. (*22*) prepared Yucca Mountain tuff thin sections amended with Pu for analysis by synchrotron-based micro−X-ray fluorescence (micro−XRF) and micro−X-ray absorption near-edge structure (XANES) spectroscopy. These measurements were performed 2 and 6 months after adding aqueous Pu(V) to the tuff. In the present work, one of the tuff thin sections was re-analyzed by XANES 2 years after the addition of aqueous Pu(V).

For the micro−XANES studies, the synchrotron hard X-ray fluorescence (XRF) microprobe on the undulator (Station ID-A) at Sector 13 of the Advanced Photon Source (Argonne National Laboratory, Argonne, IL) was used with a channel-cut Si(220) monochromator. Microfocusing optics were used to produce a small X-ray beam. A double elliptical Pt-coated Kirkpatrick−Baez mirror system angled at 2 mrad was used to focus a monochromatic undulator X-ray beam at the Pu L_{III} absorption edge (18 054 eV) to a 4 μm vertical by 7 μm horizontal beam resulting in a flux of about 10^{-10} photon s^{-1} (*25*). The thin section of tuff was contained within fitted Teflon inserts with polypropylene and Kapton windows, placed in an Al metal frame and mounted on an automated, digital x−y−z stage at 45° to the beam. Fluorescent X-rays were detected with a Si(Li) energy dispersive detector (30 mm^2 area) mounted at 90° to the incident beam and 1 cm from the sample. The Pu−XANES spectra were collected on the Lα emission line from 50 eV below the Pu absorption edge to >500 eV above the Pu absorption edge in varying step increments from 0.4 to 2.5 eV. The monochromator position and undulator were scanned simultaneously and the sample table was moved accordingly to track the position of the X-ray beam during each scan. During scanning, the change in theta (θ) for the monochromator was from 0.0015 to 0.002°. Count times varied from 1 s (PuO_2 solid and $BaPu(VI)O_6$) to 10 s (thin section) per point. Most scans were repeated from five to nine times. The spectra are normalized to the edge step and not the first absorption peak, which is often referred to as the "whiteline". The XANES edge energies were determined based on the half-height of the edge step as described by Duff et al. (*22*).

Pyrolusite Preparation. Pyrolusite (β-MnO_2) was prepared using the technique described by McKenzie (*26*). The Brunauer−Emmett−Teller (BET) surface area was measured using a nitrogen gas adsorption analyzer (ASAP 2010, Micrometrics, Inc.), and X-ray powder diffraction (XRD) spectra were obtained on a Scintag XDS2000 powder diffractometer. The point-of-zero-salt effect was determined by potentiometric titrations in 0.01, 0.05, and 0.10 M NaCl. The redox capacity in equivalents per gram of mineral, which can be related to the average Mn oxidation state, was determined via iodometric titration using the method of Carpenter (*27*) and Murray et al., (*28*). Physical and chemical characterization of the pyrolusite and detailed descriptions of the analytical methods are provided in the online Supporting Information.

Pu(IV) and Pu(V) Working Solution Preparation. A 70 μM $Pu(NO_3)_4$ stock solution (Isotope Products, Valencia, CA) was used to prepare $^{238}Pu(V)$ and $^{238}Pu(IV)$ working solutions. The ^{238}Pu accounted for >99.9% of all the Pu in the working solution. All Pu working solutions were prepared in 0.01 M NaCl. Pu(IV) solutions were prepared by evaporating an aliquot of the Pu stock solution to dryness several times in 1.0 M HNO_3. The dried residue was brought up in a small volume of 1.0 M HNO_3 then diluted to the desired Pu concentration in 0.01 M NaCl. New Pu(IV) working solutions were prepared for each experiment. Pu(V) working solutions were prepared as previously described (*29*). Oxidation state analysis was performed by parallel extraction of the Pu solution into 0.5 M thenoyltrifluoroacetone (TTA, Alfa Asear, Ward Hill, MA) in cyclohexane at pH 0.5 and 0.5 M bis-(ethyhexyl)-phosphoric acid (HDEHP; Alfa Asear, Ward Hill, MA) in heptane at pH 0.5 (*30*−*32*). A 0.5 M HDEHP solution in heptane extracts Pu(IV) and Pu(VI) from a pH ≈ 0 aqueous phase, leaving Pu(V) behind. A 0.5 M TTA solution in cyclohexane extracts Pu(IV) from a pH ≈ 0 aqueous phase, leaving Pu(V) and Pu(VI) behind. If present, Pu(III) and colloidal-Pu(IV) will also remain in the aqueous phase during the TTA extraction. However, Pu(III) is unstable under the described experimental conditions and the filtration step (discussed below) will remove any colloidal-Pu(IV) from solution. Therefore, these components are not considered during analysis. The eight Pu(IV) working solutions prepared for batch kinetic and pH adsorption edge experiment had an average purity of 94% ± 1% Pu(IV). Similarly, the Pu(V) working solutions for kinetic sorption tests and pH adsorption edge experiments contained 93% ± 5% Pu(V) and 99% ± 4% Pu(V), respectively. A complete oxidation state distribution and Pu concentration of each working solution is presented in the online Supporting Information. The oxidation state of Pu(IV) and Pu(V) working solutions (with no solid phase present) at pH 3, 5, and 8 were monitored over 30 days. These solutions showed no change in Pu(V) oxidation state. After 30 days, Pu(IV) working solutions contained 14% and 10% Pu(V) at pH 5 and 8, respectively. This is expected based upon thermodynamic considerations and the observed stability of Pu(V) in NaCl solutions (*16, 20*−*21*). ^{238}Pu concentrations were measured with an alpha−beta discriminating liquid scintillation counter (Wallac Inc., model 1415, Boston, MA). All reported Pu error was propagated from liquid scintillation uncertainties.

Oxidation State Analysis Technique. The oxidation state distribution of Pu in each sample for each reaction time was measured using a combined ultrafiltration and solvent extraction technique which is briefly described below (*15, 23, 29, 33*). First the oxidation state distribution of aqueous Pu is measured. Then the total system (solid and aqueous phase combined) Pu oxidation state distribution is measured by lowering the pH to leach Pu from the solid phase. Control experiments carrying single oxidation state Pu(IV), Pu(V), and Pu(VI) solutions through the oxidation state analysis technique verified the stability of each oxidation state during the analysis (details presented in the online Supporting Information).

For each reaction time, a 2.5-mL aliquot of the aqueous phase was removed and passed through a 12-nm filter (Microsep 30K MWCO centrifugal device; Pall Corporation, East Hills, NY). An aliquot of the filtrate was removed to determine the aqueous phase Pu concentration, and oxidation state distribution in the remaining filtrate was measured using the parallel solvent extraction technique discussed above. These data can be used to express the concentration and oxidation state distribution of Pu in the aqueous phase (eq 1).

$$[Pu]_{aq} = [Pu(IV)]_{aq} + [Pu(V)]_{aq} + [Pu(VI)]_{aq} \qquad (1)$$

The pH of the remaining sample, aqueous and solid phase, was lowered to 1.5 using $HClO_4$ and mixed for 15 min to quantitatively leach Pu(V) and Pu(VI) from the mineral surface. Quantitative leaching of Pu(V) and Pu(VI) was verified

using Np(V) and U(VI) as oxidation state analogues. A detailed discussion and data describing the use of oxidation state analogues to verify the oxidation state analysis technique are provided in the online Supporting Information. Incomplete leaching of tetravalent actinides was quantified and accounted for in the determination of the Pu oxidation state distribution by assuming that any Pu remaining on the solid phase was Pu(IV). The Pu mass balance for the total system (solid and aqueous phases combined) is expressed in eq 2:

$$m^{Pu}_{total} = [Pu(IV)]_{aq}V_{aq} + [Pu(IV)]_{solid}m_{solid} + [Pu(V)]_{aq}V_{aq} + [Pu(V)]_{solid}m_{solid} + [Pu(VI)]_{aq}V_{aq} + [Pu(VI)]_{solid}m_{solid} \quad (2)$$

where m is the mass of the solid phase (g), V is the volume of the aqueous phase (L), and [Pu(IV)], [Pu(V)], and [Pu(VI)] are the concentrations of Pu in the these oxidation states (mol/L or mol/g). Again, the $[Pu(X)]_{aq}$ parameters were measured in the aqueous phase in contact with the solid phase, and $[Pu(X)]_{solid}$ parameters were measured in the filtered pH 1.5 extracts. The Pu distribution among the three oxidation states is expressed as a fraction to account for both the solid phase and aqueous phase contributions (eq 3).

$$f^{Pu(total)}_{aq+solid} = 1.0 = f^{Pu(IV)}_{aq+solid} + f^{Pu(V)}_{aq+solid} + f^{Pu(VI)}_{aq+solid} \quad (3)$$

In some cases, the fraction of each Pu oxidation state on the solid phase was inferred by subtracting the aqueous phase Pu oxidation state distribution from the total distribution. This was done by rearranging eq 2 for $[Pu(IV)]_{solid}m_{solid}$, $[Pu(V)]_{solid}m_{solid}$, or $[Pu(VI)]_{solid}m_{solid}$ and normalizing the data by dividing each term by the total mass of Pu added. To ensure an accurate mass balance as described in eq 2, the total activity of Pu in each system was measured in fourteen randomly selected samples which were digested in a 5 M HNO_3/5M HCl solution at the end of the experiment. Pu recoveries ranged from 94% to 106%.

Batch Kinetic Experiments. Approximately 40 ± 0.4 mg of pyrolusite was added to 15-mL polypropylene centrifuge tubes. Negligible sorption of Pu to the vial walls in samples containing a solid phase was verified by washing the remaining suspension from the tube at the end of the experiment with 0.01 M NaCl then leaching any Pu with 1 M HCl. Ten-mL of a pH-adjusted, 0.01 M NaCl solution amended with 6.1×10^{-11} M Pu(V) was added to each tube to create suspensions with 10 $m^2\ L^{-1}$ (4.00 ± 0.04 g L^{-1}). Suspensions were mechanically mixed end-over-end in the dark for various reaction times and subsequently analyzed using the oxidation state analysis technique described above. Suspensions were mixed in the dark to minimize photochemically catalyzed reactions (*15, 33*). These experiments, as well as all others discussed here, were conducted on the lab benchtop and no effort was made to restrict the amount of CO_2 (gas) permitted to come into contact with the various experimental systems. CO_2 (gas) will influence the aqueous and solid phase speciation, especially as the pH increases. The pH of each sample was measured immediately prior to analysis using an Orion Triode calibrated with pH 4.01, 7.00, and 10.01 standard Orion buffer solutions. The electrode potential was measured using an Orion 420A meter.

In one experiment, 300 μm o.d. synthetic glass beads were used as the solid phase. The surface area was calculated using the reported diameter of 300 μm and assuming a spherical geometry. A calculated mass of glass was added to each sample to maintain a constant glass surface area concentration of 10 m^2L^{-1} in the suspensions throughout the experiment. The glass beads used in this work were first washed in a basic solution, then in an acidic bath to decrease the likelihood of an organic or inorganic surface contaminant.

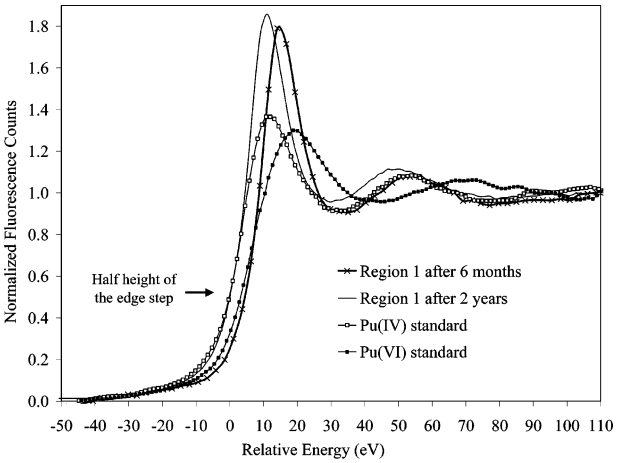

FIGURE 1. Plutonium L_3-edge XANES spectra plotted with respect to the relative XANES edge energy for sorbed Pu on YM tuff at 6 months and 2 years. All spectra taken after 2 years indicated an average oxidation state of Pu(IV); those taken after 6 months had average oxidation states predominantly of Pu(V) and Pu(VI).

Element analysis by ICP−ES indicated the glass contained 4.23 ± 0.49 μg g^{-1} Fe, 0.33 ± 0.04 μg g^{-1} Mn, and 99.6 ± 10.0 μg g^{-1} Pb.

pH Adsorption Edge Experiments. Batch experiments to determine sorption as a function of pH were conducted with pyrolusite. Mineral suspensions of 10 $m^2\ L^{-1}$ were prepared which spanned the pH range 2−8 in 0.5 pH unit increments with 0.01 M NaCl as a backing electrolyte. The amount of acid or base added was small (maximum of 1% based on simple volume and molarity calculations) with respect to the ionic strength of the background electrolyte. The samples were mechanically mixed in the dark and pH adjusted daily with 0.1 M HCl or 0.1 M NaOH. After the pH remained stable for several days, an aliquot of a Pu(IV) or Pu(V) working solution was added to yield an initial Pu concentration of 5.0 $\times 10^{-11}$ M, and the samples were returned to the mechanical mixer. pH was measured every 4 days and adjusted if necessary. After 30 days, the samples were analyzed using the total system oxidation state analysis technique described above.

Results and Discussion

Plutonium Interactions with Yucca Mountain Tuff. Using micro−XANES, Duff et al. (*22*) observed oxidation of Pu(V) to Pu(VI) following sorption to a natural zeolitic tuff from Yucca Mt. The tuff contained trace quantities of manganese oxides and more abundant Fe-oxide phases. Elemental maps generated with micro−XRF imaging demonstrated that Pu was preferentially associated with Mn oxides (specifically, ranciete, $(Ca,Mn)OMn^{IV}O_2{\cdot}3H_2O$, an iso-structural form of birnessite, with Ca as the dominant cation in the interlayer) and co-associated smectites rather than with iron oxides or zeolites. These measurements were performed 2 and 6 months after adding aqueous Pu(V) to the tuff. In the present work, the tuff thin sections were reanalyzed by XANES 2 years after the addition of aqueous Pu(V). As shown in Figure 1, the predominant solid-phase species after 2 years is Pu(IV). Additionally, the Pu is still found to be associated with the mineral phases containing Mn, having an estimated loading of 2000 mg Pu kg^{-1} at the Mn-rich regions on the tuff. Therefore, the Pu(V) initially equilibrated with Yucca Mountain tuff was oxidized to Pu(VI) or remained unchanged and then reduced to Pu(IV) over time. These data from aged samples appear to conflict with observations that Mn(IV)-containing minerals are capable of oxidizing Pu (*15, 23*).

Kinetic Studies of Pu Interactions with Pyrolusite and Glass Beads. To further examine interactions of Pu with Mn

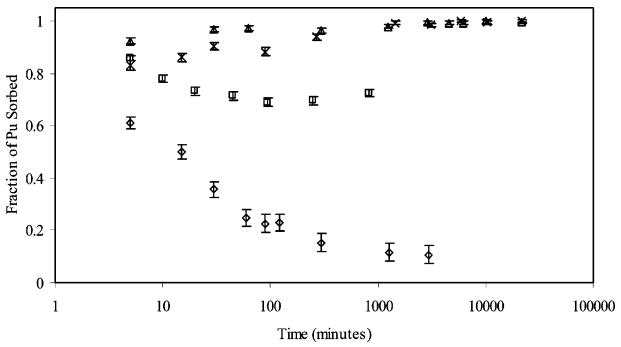

FIGURE 2. Fraction of sorbed Pu versus time in 10 m^2 L^{-1} (4.00 ± 0.04 g L^{-1}) pyrolusite suspensions at varying pH levels. Symbols: (◇) pH 2.6, (□) pH 3.4, (△) pH 4.8, (×) pH 8.2. System Parameters: [NaCl] = 0.01 M; initially added Pu(IV) at [Pu] = 6.1 × 10^{-11} M; error bars based upon propagation of liquid scintillation counting uncertainties.

oxides, batch sorption experiments were designed to study the interactions between Pu and a synthetic Mn(IV) mineral, pyrolusite, as a function of time and bulk solution pH. A plot of Pu (initially Pu(IV)) sorbed versus time over the pH range 2.6−8.2 in pyrolusite suspensions is presented in Figure 2. At all pH values, a large fraction of the Pu was sorbed within 5 min, ranging from 0.6 at pH 2.6 to >0.8 at pH 8.2. The initial sorption phase was followed by a period of Pu desorption at the pH values of 2.6 and 3.4 and continual slow uptake at pH 4.8 and 8.2. Nearly complete sorption of all Pu occurred after 7 days at pH 4.8 and 8.2.

Insight into the processes responsible for these observations can be gleaned from Pu oxidation state analyses over time in the pH 2.6 and 8.2 systems (Figure 3). The plutonium oxidation state in the aqueous phase and total system (aqueous and solid phase combined) of the pH 2.6 and 8.2 systems were monitored over time using the techniques described in the Materials and Methods section. Oxidation of Pu(IV) at pH 2.6 occurs with a steady decline of Pu(IV) and corresponding increases in Pu(V) and Pu(VI) (Figure 3a). During these experiments, no Pu(IV) was detected in the aqueous phase of the suspensions (data not shown), suggesting that Pu(IV) was oxidized on the pyrolusite surface and subsequently partitioned into the aqueous phase as Pu(V/VI) at pH 2.6. The decrease in the fraction of Pu sorbed (Figure 2) and the increase in the fraction of Pu(V/VI) in the system over time (Figure 3a) indicate that oxidation to Pu(V/VI) was followed by desorption.

Immediately following Pu(IV) addition to the pyrolusite suspension at pH 8.2, there was a slight increase in the fraction of Pu(V) and Pu(VI) (Figure 3b). During the first 60 min of reaction and while Pu(V) and Pu(VI) were present, a small fraction of Pu desorbed into the aqueous phase. Similar to the suspension equilibrations at pH 2.6, no Pu(IV) was measured in the aqueous phase, indicating a surface mediated reaction. With time, however, the oxidized Pu repartitioned to the pyrolusite surface and was rereduced to Pu(IV). These data lead us to conclude that Pu in the aqueous phase of a pyrolusite suspension will be Pu(V/VI) and Pu sorbed to the solid phase will be Pu(IV). These results are consistent with the XANES analysis of the oxidation state distribution of sorbed Pu to natural Mn(IV) phases within Yucca Mountain tuff (Figure 1). The enhanced reaction rates in the pyrolusite study, as compared to the tuff samples, may be due to a number of experimental and mineralogical processes, such as the appreciably greater surface area and better mixing achieved in the pyrolusite study. A kinetic study, similar to those described using pyrolusite, was repeated using synthetic glass beads and a Pu(V) amendment (the pyrolusite system received Pu(IV)). Although the reaction kinetics were much

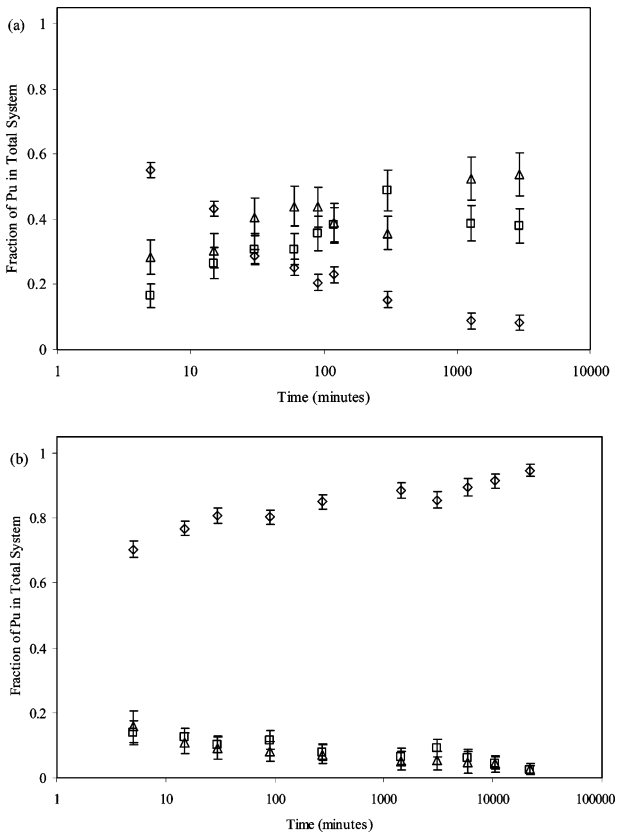

FIGURE 3. Total system Pu oxidation state distribution in 10.0 ± 0.1 m^2 L^{-1} (4.00 ± 0.04 g L^{-1}) pyrolusite suspensions at (a) pH 2.59 ± 0.04 and (b) pH 8.22 ± 0.04. Symbols: (◇) Pu(IV), (□) Pu(V), (△) Pu(VI); error bars based upon propagation of liquid scintillation counting uncertainties. System parameters: [NaCl] = 0.01 M; initially added Pu(IV) at [Pu] = 6.1 × 10^{-11} M).

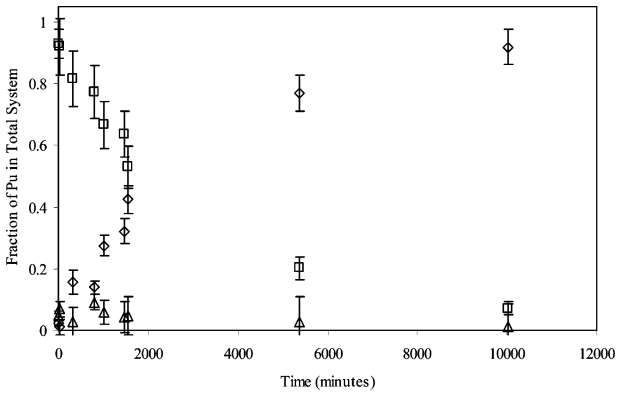

FIGURE 4. Total system Pu oxidation state distribution changes when in contact with glass. Symbols: (◇) Pu(IV), (□) Pu(V), (△) Pu(VI); error bars based upon propagation of liquid scintillation counting uncertainties. System parameters: pH 8.19 ± 0.05; [glass] = 10.4 ± 0.3 m^2 L^{-1}(1.34 ± 0.04 g L^{-1}); [NaCl] = 0.01 M; initially added Pu(V) at $[Pu]_{total}$ = 6.1 × 10^{-11} M.

slower, the changes in Pu oxidation states were very similar to those observed for pyrolusite (Figure 4). There was a decrease in the fraction of Pu(V) in the system with a corresponding increase in the fraction of Pu(IV), indicating that Pu(V) was being reduced. Analysis of Pu in the aqueous phase showed no Pu(IV), indicating that reduction in the system did not occur until Pu was sorbed to the glass beads. Trace Fe in the glass, may have been an electron source for Pu(V) reduction and hydroxide sites on the glass surface may have stabilized Pu(IV) as a hydroxide species. The reduction of Pu(V) by glass observed in these experiments is similar to

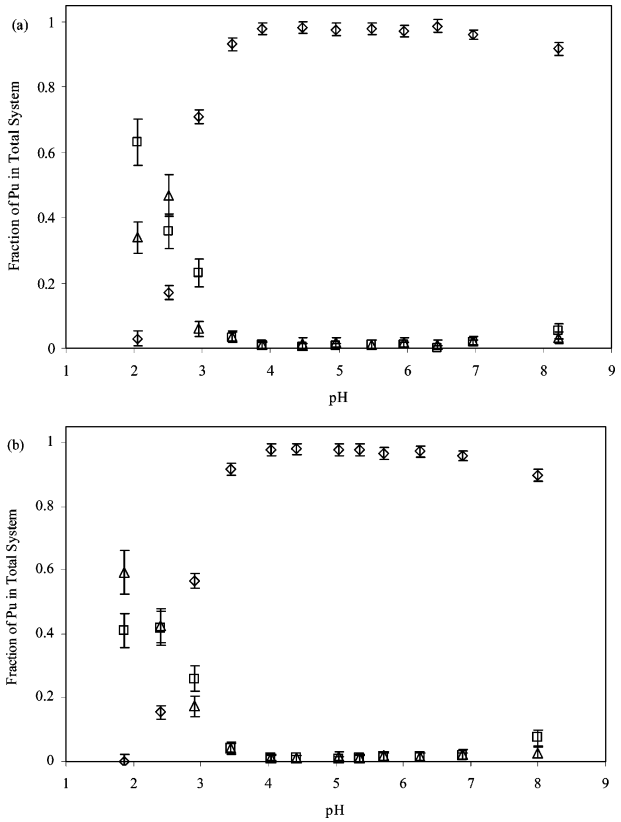

FIGURE 5. Total system (aqueous and solid phases oxidation state distribution versus pH after 30 days in (a) initially Pu(IV) and (b) initially Pu(V) pyrolusite systems. Symbols: (◇) Pu(IV), (□) Pu(V), (△) Pu(VI); error bars based upon propagation of liquid scintillation counting uncertainties. System parameters: $[Pu]_{total} = 6.1 \times 10^{-11}$ M; [pyrolusite] = 9.9 ± 0.3 m^2 L^{-1} (3.92 ± 0.05 g L^{-1}); [NaCl] = 0.01 M.

the observation by Kersting et al. (*13*) of Pu(V) reduction by SiO_2 using XANES. These are independent observations using different techniques, both of which show the reduction of sorbed Pu(V/VI) to Pu(IV) surface species.

Equilibrium Studies of Plutonium Interactions with Pyrolusite. Sorption experiments as a function of pH were conducted to provide information about the Pu oxidation state distribution after 30 days of equilibration in pyrolusite suspensions amended with Pu(IV) or Pu(V). Data describing the Pu oxidation state distribution in the total system and solid phase are presented in Figure 5. The data sets are nearly identical, irrespective of whether Pu(IV) or Pu(V) was initially added, indicating that steady state had been achieved. The pH sorption edge occurs around pH 3 (online Supporting Information). Below this pH, all the aqueous Pu was in the +5 and +6 oxidation states (data not shown) and a majority of the solid phase Pu was also in the +5 and +6 form. Above pH 3, Pu in the solid phase was almost entirely in the +4 state, again, irrespective of whether Pu(IV) or Pu(V) was initially added to the system. Therefore, at pH values below the sorption edge, Pu was oxidized and partitioned into the aqueous phase and at pH values above the sorption edge, >95% of the total Pu was sorbed and Pu(IV) was the predominant oxidation state.

The redox capacity of the pyrolusite used in these experiments was measured by an iodometric titration method (*27, 28*). The redox capacity, which can be related to the average Mn oxidation state, was $2.41 \pm 0.11 \times 10^{-2}$ equivalents g^{-1}. This corresponds to a O:Mn ratio of 1.95 ± 0.03, instead of the ideal ratio of 2.00. Therefore, some Mn(II) or Mn(III) may have been present in the pyrolusite, providing an electron source for the reduction reaction with Pu(V/VI). Because only trace Pu concentrations ($[Pu]_{total} = 6.1 \times 10^{-11}$ M) were used in these experiments, only trace Mn(II) or Mn(III) substitutions would be necessary to provide sufficient amount of electrons for the reduction reaction. Manganese typically exists in multiple oxidation states in natural and anthropogenic minerals (*34*). Additionally, it is noteworthy that pyrolusite is a semiconductor with a band gap approximately 1 order of magnitude lower than that of hematite (*35*) and may be capable of transporting electrons through the mineral lattice as discussed for iron (oxyhydr)oxides (*35*–*36*). The effects of semiconductor properties in these systems could be similar to that proposed in describing Pu interactions with goethite and hematite (*33*).

Disproportionation of Pu(V) or Pu(IV) is not considered to significantly effect the Pu oxidations state distribution in these systems because of the low total Pu concentration. In acidic conditions, Pu(V) can disproportionate to form Pu(IV) and Pu(VI) if the initial Pu(V) concentration is sufficiently high. The reaction is as follows (*37*):

$$2Pu(V)O_2^{+} + 4H^{+} \leftrightarrow Pu(VI)O_2^{2+} + Pu(IV)^{4+} + 2H_2O \quad (4)$$

The rate of disproportionation depends on the square of the Pu concentration and, therefore, decreases rapidly as Pu approaches tracer levels. Additionally, Pu(V) disproportionation has a fourth power dependence on the hydrogen ion concentration and is therefore favored in acidic solutions. Disproportionation of Pu(IV) occurs through the reaction (*38*):

$$3Pu(IV)^{4+} + 2H_2O \leftrightarrow 2\ Pu(III)^{3+} + Pu(VI)O_2^{2+} + 4H^{+} \quad (5)$$

Pu(IV) disproportionation has a third power dependence on the Pu concentration and will therefore proceed very slowly at tracer level Pu concentrations. The Pu(III) noted in eq 2 would be unstable and likely oxidized by water at the circumneutral pH values where the experiments were conducted. The stability of Pu(V) and Pu(IV) in the working solutions over time demonstrates that disporportionation is not significant over the time period of these experiments. However, as Pu is attracted to a mineral surface, the local concentration within the electrical double layer will be higher than that of the bulk solution. The effects of this concentration gradient on Pu disproportionation have not been examined.

Possible Reaction Mechanisms. The ability of birnessite, pyrolusite, and other Mn(III,IV)-containing minerals to oxidize other metal species has been shown by a number of researchers (*15, 23, 39*–*43*). Despite the observed oxidizing nature of Mn minerals, this work has shown that Pu(IV) is the stable oxidation state of Pu sorbed to some Mn(IV) oxide minerals. Several other researchers have observed reduction of Pu on Mn containing minerals. Following the addition of Pu(V) to birnessite solutions, Keeney-Kennicutt and Morse (*15*) observed Pu(IV), Pu(V), and Pu(VI) on the mineral surface. They attributed the observed oxidation of Pu to interaction with Mn(IV). The authors did not comment on the large fractions of Pu(IV) observed following addition of Pu(V) to a birnessite suspension. Shaughnessy et al. (*24*) observed reduction of plutonium on hausmannite (Mn_3O_4) and manganite (γ-MnOOH) surfaces. Kersting et al. (*13*) observed Pu(IV) as the predominant solid-phase oxidation state on both pyrolusite and birnessite.

The stability of Pu(IV) is proposed to be due to the formation of a stable hydrolyzed Pu(IV) surface species. An explanation may lie in a discussion from Morgenstern and Choppin (*23*), who were studying oxidation of Pu(IV) by a synthetic manganese dioxide (MnO_2, crystalline structure unknown). They observed that Pu(IV) was oxidized to Pu(V)

and Pu(VI) at low pH (2.0−3.5), but oxidation was inhibited at high pH (8.0) values. Inhibition of oxidation at higher pH was attributed to the stabilization of Pu(IV) as the fully hydrolyzed species $Pu(OH)_4$(aq). Significant amounts of $Pu(OH)_4$ (aq) have been shown to be present at pH values as low as 4 (*1*). Since hydrolysis will change the redox potential of a given Pu species, Pu reduction on a mineral surface is dependent on both Pu speciation/hydrolysis at the mineral surface as well as the redox capacity of the surface. It is possible that hydrolysis of surface bound Pu(IV) may sufficiently alter the reduction potential such that reoxidation of Pu(IV) by Mn(IV) is not energetically favorable. This mechanism by which the hydrolysis and sorption of Pu changes the free energy to provide a barrier against reoxidation by Mn(IV) may be somewhat similar to that put forth by Wan et al. (*44*), who observed the reoxidation of bioreduced U under reducing conditions. Microbial respiration produced (bi)carbonate and reoxidation of U purportedly occurred due to the thermodynamic stability of U(VI) carbonate complexes, although microbially mediated U(VI) reduction to U(IV) was initially observed and the microbial reducing community was sustained throughout the experiment.

The oxidation and reduction of Pu observed in these systems likely occurred through different reaction pathways. The effective charge for Pu species decreases in the order $Pu(IV)^{+4}$, $Pu(VI)O_2^{+2}$, $Pu(V)O_2^{+}$; making Pu(IV) more surface active compared to Pu(V). McCubbin and Leonard (*45*) observed competitive sorption between Ca^{2+} and Mg^{2+} cations with Pu(V), while similar effects of Pu(IV) sorption were not observed. These data indicate sorption of Pu(V) likely occurs through formation of outer-sphere complexes while Pu(IV) forms inner-sphere complexes. These two adsorption mechanisms likely have a significant impact on Pu oxidation state transformations. Oxidation of Pu by Mn-bearing minerals appears to be favored as long as the oxidized species is desorbed from the mineral surface or weakly electrostatically adsorbed. This occurs at low pH levels where the pyrolusite surface carries a net positive charge which will repel the cationic Pu(V) and Pu(VI) species. As the pH increases and the negative surface charge increases, Pu will be attracted to the surface where redox reactions may occur. Interactions between the strongly hydrolyzable Pu(IV) cation or free $Pu(V)O_2^{+}$ cation with mineral surfaces may result in the formation of a stable Pu(IV)-hydroxide surface complex. Hydrolysis of a Pu(IV) surface complex (following or coincident with Pu(V) reduction), coupled with the eventual loss of water from the hydration sphere upon formation of a Pu(IV) surface complex, may provide a barrier to Pu(IV) reoxidation. Therefore, Pu(IV) hydrolysis may be the driving force for the observed stability of Pu(IV) on the mineral surface. This is supported by the observation of Pu(V) reduction on glass beads as well as the stability of Pu(IV) on an oxidizing surface such as pyrolusite.

The proposed mechanisms in this work are supported by the observations that (1) regardless of the initial aqueous Pu oxidation state added to a system, similar oxidation state distributions were obtained after 30 days of contact in pyrolusite suspensions, (2) initial oxidation followed by reduction was observed in pyrolusite and tuff systems, (3) reduction of Pu(V) was observed in pyrolusite suspensions despite the observed oxidizing capacity of Mn(IV) oxides, and (4) Pu(V) or Pu(VI) remaining on the solid phase of both tuff and synthetic pyrolusite are eventually reduced to Pu(IV). The proposed mechanisms are largely speculative, based on long-term experimental observations and theoretical thermodynamic considerations. To truly describe the interfacial reactions occurring in these systems, techniques capable of investigating the mineral−water interface in real-time are required. That Mn(IV) minerals can oxidize Pu(IV) to the more mobile Pu(V/VI) forms has required regulators and risk assessors to assume that Pu emplaced at some geological waste repositories will be more mobile than may, in fact, be the case. This study lends itself to a new conceptual model describing Pu geochemistry that can be used to more accurately predict the risk associated with the disposal of Pu-containing waste.

Acknowledgments

This research was supported in part by the South Carolina Universities Research and Education Foundation (SCUREF) under the U.S. Department of Energy (DOE) contract DE-FC09-00SR22184—Cooperative Agreement DOES0015, "Radiochemistry Education Award Program (REAP II)". Additionally, this work was supported in part by DOE's Environmental Management Science Program (EMSP). Portions of this work were performed at GeoSoilEnviro-CARS (GSE-CARS), Sector 13, Advanced Photon Source (APS). Use of the APS was supported by the DOE, Basic Energy Sciences, Office of Energy Research, under contract no. W-31-109-Eng-38. The research was also supported by Financial Assistance Award no. DE-FC09-96SR18546 from the DOE to the University of Georgia Research Foundation. We also thank the associate editor and four anonymous reviewers for their helpful comments.

Supporting Information Available

Data demonstrating leaching of the oxidation state analogues from pyrolusite and other experimental controls used in the oxidation state analysis technique; physical and chemical characterization of pyrolusite; additional Pu oxidation state distribution data in pyrolusite suspensions at pH 3.4. This material is available free of charge via the Internet at http://pubs.acs.org.

Literature Cited

(1) Morse, J. W.; Choppin, G. R. The chemistry of transuranic elements in natural waters. *Rev. Aquat. Sci.* **1991**, *4*(1), 1−22.
(2) Silva, R. J.; Nitsche, H. Actinide environmental chemistry. *Radiochim. Acta* **1995**, *70/71*, 377−396.
(3) Neu, M. P.; Icopini, G. A.; Boukhalfa, H. Plutonium speciation affected by environmental bacteria. *Radiochim. Acta* **2002**, *93*, 705−715.
(4) Panak, P. J.; Nitsche, H. Interaction of aerobic soil bacteria with plutonium(VI). *Radiochim. Acta* **2001**, *89*, 499−504.
(5) Panak, P. J.; Cooth, C. W.; Caulder, D. L.; Bucher, J. J.; Shuh, D. K.; Nitsche, H. X-ray absorption fine structure spectroscopy of plutonium complexes with *Bacillus sphaericus*. *Radiochim. Acta* **2002**, *90*, 315−321.
(6) Prout, W. E. Adsorption of fission products by Savannah River plant soil. *Soil Sci.* **1958**, *86*, 13−17.
(7) Kaplan, D. I.; Powell, B. A.; Demirkanli, D. I.; Fjeld, R. A.; Molz, F. J.; Serkiz, S. M.; Coates, J. T. Influence of oxidation states on plutonium mobility during long-term transport through an unsaturated subsurface environment. *Environ. Sci. Technol.* **2004**, *38*, 5053−5058.
(8) Kaplan, D. I.; Demirkanli, D. I.; Gumapas, L.; Powell, B. A.; Fjeld, R. A.; Molz, F. J.; Serkiz, S. M. 11-Year Field Study of Pu Migration from Pu III, IV, and VI Sources. *Environ. Sci. Technol.* **2006**, *40*, 443−448.
(9) Cleveland, J. M. *The Chemistry of Plutonium;* American Nuclear Society: La Grange Park, IL, 1979.
(10) Weigel, F.; Katz, J. J.; Seaborg, G. T. In *The Chemistry of the Actinide Elements;* Katz, J. J., Seaborg, G. T., Morss, L. R., Eds.; Chapman & Hall: New York, 1986; Vol. 1, pp 680−702.
(11) Choppin, G. R. Actinide speciation in the environment. *Radiochim. Acta* **2003**, *91*, 645−649.
(12) Runde, W.; Conradson, S. D.; Efurd, D. W.; Lu, N.; VanPelt, C. E.; Tait, C. D. Solubility and sorption of redox-sensitive radionuclides (Np, Pu) in J-13 water from the Yucca Mountain site: comparison between experimental and theory. *App. Geochem.* **2002**, *17*, 837−853.
(13) Kersting, A. B.; Zhao, P.; Zavarin, M.; Sylwester, E. R.; Allen, P. G.; Williams, R. W. Chapter 5: sorption of Pu(V) on mineral colloids. In *Colloidal-Facilitated Transport of Low-Solubility Radionuclides: A Field, Experimental, and Modeling Investiga-*

tion, report UCRL-ID-149688; Kersting A. B.; Reimus, P. W. Eds.; Lawrence Livermore National Laboratory: Livermore, CA.
(14) Kersting, A. B.; Efurd, D. W.; Finnegan, D. L.; Rokop, D. J.; Smith, D. K.; Thompson, J. L. Migration of plutonium in groundwater at the Nevada Test Site. *Nature* **1999**, *397*, 56−59.
(15) Keeney-Kennicutt, W. L.; Morse, J. W. The redox chemistry of $Pu(V)O_2^+$ interactions with common mineral surfaces in dilute solutions and seawater. *Geochim. Cosmochim. Acta* **1985**, *49*, 2577−2588.
(16) Sanchez, A. L.; Murray, J. W.; Sibley, T. H. The adsorption of plutonium IV and V on goethite. *Geochim. Cosmochim. Acta* **1985**, *49*, 2297−2307.
(17) Penrose, W. R.; Metta, D. N.; Hylko, J. M.; Rinckel, L. A. The reduction of plutonium(V) by aquatic sediments. *J. Environ. Radioact.* **1987**, *5*, 169−184.
(18) Nelson, D. M.; Lovett, M. B. Oxidation state of plutonium in the irish sea. *Nature* **1978**, *276*, 599−601.
(19) Mitchell, P. E.; Battle, J. V.; Downes, A. B.; Bondren, O. M.; Vintro, L. L.; Sanchez-Cabeza, J. A. Recent observations on the physicochemical speciation of plutonium in the Irish Sea and the Western-Mediterranean. *Appl. Radiat. Isot.* **1995**, *46*(11), 1175.
(20) Orlandini, K. A.; Penrose, W. R.; Nelson, D. M. Pu(V) as the stable form of oxidized plutonium in natural waters. *Mar. Chem.* **1986**, *18*, 49−57.
(21) Nitsche, H.; Roberts, K.; Xi, R.; Prussin, T.; Becraft, K.; Mahamid, I. A.; Silber, H. B.; Carpenter S. A.; Gatti, R. C. Long-term plutonium solubility and speciation studies in a synthetic brine. *Radiochim. Acta* **1994**, *66/67*, 3−8.
(22) Duff, M. C.; Hunter, D. B.; Triay, I. R.; Bertsch, P. M.; Reed, D. T.; Sutton, S. R.; Shea-McCarthy, G.; Kitten, J.; Eng, P.; Chipera, S. J.; Vaniman, D. T. Mineral associations and average oxidation states of sorbed Pu on tuff. *Environ. Sci. Technol.* **1999**, *33*, 2163−2169.
(23) Morgenstern, A.; Choppin, G. R. Kinetics of the oxidation of Pu(IV) by manganese oxide. *Radiochim. Acta* **2002**, *90*, 69−74.
(24) Shaughnessy, D. A.; Nitsche, H.; Booth, C. H.; Shuh, D. K.; Waychunas, G. A.; Wilson, R. E.; Gill, H.; Cantrell, K. J.; Serne, R. J. Molecular interfacial reactions between Pu(VI) and manganese oxide minerals manganite and hausmannite. *Environ. Sci. Technol.* **2003**, *37*(15), 3367−3374.
(25) Eng, P. J.; Rivers, M. L.; Yang, B. X.; Schildkamp, W. Microfocusing 4-keV to 65-keV X-rays with bent Kirkpatrick-Baez mirrors *Proc. SPIE* **1995**, *25*(16), 41−51.
(26) McKenzie, R. M. The synthesis of birnessite, cryptomelane, and some other oxides and hydroxides or manganese. *Mineral. Mag.* **1971**, *38*, 493−502.
(27) Carpenter, J. H. The Chesapeake Bay Institute technique for the Winkler dissolved oxygen method. *Luminology Oceanogr.* **1965**, *10*(1), 141−143.
(28) Murray, J. W.; Balistrieri, L. S.; Paul, B. The oxidation state of manganese in marine sediments and ferromanganese nodules. *Geochim. Cosmochim. Acta* **1984**, *48*, 1237−1247.
(29) Powell, B. A.; Fjeld, R. A.; Kaplan, D. I.; Coates, J. T.; Serkiz, S. M. $Pu(V)O_2^+$ adsorption and reduction by synthetic magnetite (Fe_3O_4). *Environ. Sci. Technol.* **2004**, *38*, 6016−6024.
(30) Bertrand, P. A.; Choppin, G. R. Separation of actinides in difference oxidation states by solvent extraction. *Radiochim. Acta* **1982**, *31*, 135−137.
(31) Kobashi, A.; Choppin, G. R.; Morse, J. W. A study of techniques for separating plutonium in different oxidation states. *Radiochim. Acta* **1988**, *43*, 211−215.
(32) Neu, M. P.; Hoffman, D. C.; Roberts, K. E.; Nitsche, H.; Silva, R. J. Comparison of chemical extractions and laser photoacoustic spectroscopy for determination of plutonium species in near-neutral carbonate solutions. *Radiochim. Acta* **1994**, *66*, 265−272.
(33) Powell, B. A.; Fjeld, R. A.; Kaplan, D. I.; Coates, J. T.; Serkiz, S. M. $Pu(V)O_2^+$ adsorption and reduction by synthetic hematite (α-Fe_2O_3) and goethite (α-FeOOH). *Environ. Sci. Technol.* **2005**, *39*, 2107−2114.
(34) McKenzie. R. M. Manganese Oxides and Hydroxides. In *Minerals in Soil Environments*, 2nd ed.; Dixon, J. B., Weed, S. B., Eds.; Soil Science Society of America: Madison, WI, 1989; pp 439−466.
(35) Waite, T. A. Photoredox processes at the mineral-water interface. In *Mineral-Water Interface Geochemistry*; Hochella, M. F., White A. F., Eds.; Mineralogical Society of America: Washington, DC, 1990; Vol. 23, pp 559−601.
(36) Williams, A. G. B.; Scherer, M. M. Spectroscopic evidence for Fe(II)-Fe(III) electron transfer at the iron oxide-water interface. *Environ. Sci. Technol.* **2004**, *38*, 4782−4790.
(37) Rabideau, S. W. The Kinetics of the Disproportionation of Pu-(V). *J. Am. Chem. Soc.* **1957**, *79*, 6350−6353.
(38) Rabideau, S. W. Equilibria and Reaction Rates in the Disproportionation of Pu(IV). *J. Am. Chem. Soc.* **1952**, *75*, 798−801.
(39) Fredrickson, J. K.; Zachara, J. M.; Kennedy, D. W.; Liu, C.; Duff, M. C.; Hunter, D. B.; Dohnalkova, A. Influence of Mn oxides on the reduction of uranium(VI) by the metal reducing bacterium *shewanella putrefaciens*. *Geochim. Cosmochim. Acta* **2002**, *66*(18), 3247−3262.
(40) Weaver, R. M.; Hochella, M. F.; Ilton, E. S. Dynamic processes occurring at the Cr(III) manganite (γ-MnOOH) interface: Simultaneous adsorption, microprecipitation, oxidation/reduction, and dissolution. *Geochim. Cosmochim. Acta* **2002**, *66*(23), 4119−4132.
(41) Jardine P. M.; Taylor D. L. Kinetics and mechanisms of Co-(II)EDTA oxidation by pyrolusite. *Geochim. Cosmochim. Acta* **1995**, *59*(20), 4190−4203.
(42) Scott, M. J.; Morgan, J. J. Reactions at oxide surfaces. 1. Oxidation of As(III) by synthetic birnessite. *Environ. Sci. Technol.* **1995**, *29*, 1898−1905.
(43) Scott, M. J.; Morgan J. J. Reactions at oxide surfaces. 2. Oxidation of Se(IV) by synthetic birnessite. *Environ. Sci. Technol.* **1996**, *30*, 1990−1996.
(44) Wan, J.; Tokunaga, T. K.; Brodie, E.; Wang, Z.; Zheng, Z.; Herman, D.; Hazen, T. C.; Firestone, M. K.; Sutton, S. R. Reoxidation of bioreduced uranium under reducing conditions. *Environ. Sci. Technol.* **2005**, *59*, 6162−6169.
(45) McCubbin, D.; Leonard, K. S. A preliminary study to assess the effect of some seawater components on the speciation of plutonium. *J. Radioanal. Nucl. Chem.* **1993**, *172*(2), 363−370.

Received for review November 22, 2005. Revised manuscript received April 5, 2006. Accepted April 5, 2006.

ES052353+